

International Journal of Modern Physics D
 © World Scientific Publishing Company

**Stable TeV - Black Hole Remnants at the LHC:
 Discovery through Di-Jet Suppression, Mono-Jet Emission and a Supersonic
 Boom in the Quark-Gluon Plasma**

H. Stöcker

*FIAS- Frankfurt Institute for Advanced Studies
 and
 Institut für Theoretische Physik, Johann Wolfgang Goethe - Universität,
 Max - von - Laue - Str. 1,
 D-60438 Frankfurt am Main, Germany
 E-mail: stoecker@FIAS.uni-frankfurt.de*

Received Day Month Year
 Revised Day Month Year
 Communicated by Managing Editor

The production of Large Extra Dimension (LXD) Black Holes (BHs), with a new, fundamental mass scale of $M_f = 1$ TeV, has been predicted to occur at the Large Hadron Collider, LHC, with the formidable rate of 10^8 per year in p-p collisions at full energy, 14 TeV, and at full luminosity.

We show that such LXD-BH formation will be experimentally observable at the LHC by the complete disappearance of all very high p_t (> 500 GeV) back-to-back correlated Di-Jets of total mass $M > M_f = 1$ TeV, in the large detectors ALICE, ATLAS and CMS.

We suggest to complement this clear cut-off signal at $M > 2 * 500$ GeV in the di-jet-correlation function by detecting the subsequent, Hawking-decay products of the LXD-BHs, namely either multiple high energy (> 100 GeV) SM Mono-Jets (i.e. away-side jet missing), sprayed off the evaporating BHs isentropically into all directions or the thermalization of the multiple overlapping Hawking-radiation in a Heckler-Kapusta-Plasma: The extreme energy density of the Hawking Radiation may yield a Heckler-Kapusta-Hawking Quark-Gluon Plasma of SM - and SUSY - particles at temperatures above the electroweak phase transition, which hydrodynamically (isentropically) evolves and cools until the Quark-Hadron phasetransition and chemical freezeout at $T \sim 100$ MeV is reached. Microcanonical quantum statistical calculations of the Hawking evaporation process for these LXD-BHs show that cold black hole remnants (BHRs) of Mass $\sim M_f$ remain leftover as the ashes of these spectacular Di-Jet-suppressed events. The BHRs are charged and can be detected as a track in the Central TPC of ALICE.

Strong Di-Jet suppression is also expected with Heavy Ion beams at the LHC, due to Quark-Gluon-Plasma induced jet attenuation at medium to low jet energies, $p_t < 200$ GeV. The (Mono-)Jets in these events can be used to trigger for Tsunami-emission of secondary compressed QCD-matter at well defined Mach-angles, both at the trigger side and at the awayside (missing) jet. The Machshock-angles allow for a direct measurement of both the equation of state EoS and the speed of sound c_s via supersonic bang in the "big bang" matter.

We discuss the importance of the underlying strong collective flow - the gluon storm - of the QCD- matter for the formation and evolution of these Machshock cones. We predict a significant deformation of Mach shocks from the gluon storm in central Au+Au collisions

2 *H. Stöcker*

at RHIC and LHC energies, as compared to the case of weakly coupled jets propagating through a static medium. A possible complete stopping of $p_t > 50$ GeV jets at the LHC in 2-3 fm yields nonlinear high density Mach shocks in the quark gluon plasma, which can be studied in the complex emission and disintegration pattern of the possibly supercooled matter. We report on first full 3-dimensional fluid dynamical studies of the strong effects of a first order phase transition on the evolution and the Tsunami-like Mach shock emission of the QCD matter.

Keywords: LHC, black holes, Mach Shocks

1. Introduction

The Frankfurt-born Astronomer Karl Schwarzschild discovered the first analytic solution of the General Theory of Relativity ¹. He laid the ground for studies of some of the most fascinating and un-understood objects in the universe, the Schwarzschild Black Holes. Recently it was conjectured that Black Holes (BHs) do also reach into the regime of particle and collider physics: In the presence of additional compactified large extra dimensions (LXDs), it seems possible to produce tiny black holes at the LHC (Large Hadron Collider at the European Center for Nuclear Research, CERN, Geneva). This allows for tests of Planck scale physics and of the onset of quantum gravity in the laboratory. Understanding black hole physics is a key to the phenomenology of these new effects beyond the Standard Model (SM).

The presence of additional spacelike dimensions ², on top of our usual three space dimensions, seems ruled out by experience, but these additional dimensions are compactified to small radii, which explains why we have not yet noticed them.

During the last decade, several models ^{3,4} using compactified LXDs as an additional assumption to the quantum field theories of the Standard Model (SM) have been proposed. The setup of these effective models is motivated by String Theory, though the question whether our spacetime has additional dimensions is well-founded on its own and worth the effort of examination.

The models with LXDs provide us with a useful description to predict first effects beyond the SM. They do not claim to be first principles theories. Instead, their simplified framework allows the derivation of testable results, which can in turn help us to gain insights about the underlying theory.

Large extra dimensions have e.g. been incorporated into the framework of the SM by the ADD-model proposed by Arkani-Hamed, Dimopoulos and Dvali ³, who add d extra spacelike dimensions without curvature, in general each of them compactified to the same radius R . All SM particles are confined to our 3+1 brane, while gravitons are allowed to propagate freely in the 3+d+1 dimensional bulk. In the following, we consider the phenomenological consequences of the ADD- model ³ with a new fundamental mass-scale M_f . The new and the apparent Planck scales are related by

$$m_p^2 = M_f^{d+2} R^d. \quad (1)$$

The radius R of these extra dimensions, for $M_f \sim \text{TeV}$, can be estimated with Eq.(1) and typically lies in the range from 10^{-1} mm to ~ 100 fm for d from 2 to 7.

Therefore, the inverse compactification radius $1/R$ lies in energy range eV to MeV, respectively. The case $d = 1$ is excluded. It would result in an extra dimension about the size of the solar system. $d=2$ has recently been excluded by Cavendish-type experiments.

2. Estimate of LXD- Black Hole formation crosssections at the LHC

The most exciting signature of LXDs is the possibility of black hole production as discussed in the present note ⁵⁻²¹ and in ultra high energetic cosmic ray events ^{22,23}. For recent updates on constraints on the parameters d and M_f see e.g. ²⁴. In the standard $3 + 1$ dimensional space-time, the production of black holes requires a concentration of energy-density which can not be reached in the laboratory, while in the higher dimensional space-time, gravity becomes stronger at small distances, and, therefore, the event horizon is located at a larger radius, $R_H \sim 10^{-4} fm$.

We are interested in the case where the black hole has a mass close to the new fundamental scale $M_{BH} \approx M_f \approx 1$ TeV. This corresponds to a radius $R_S = R_{BH} = R_H \approx 10^{-4} fm$ close to the inverse new fundamental scale M_f , and thus $R_H \ll R$.

Higher dimensional Schwarzschild-metrics have been derived in ²⁵ with the Schwarzschildradii R_H

$$R_H^{d+1} = \frac{2}{d+1} \left(\frac{1}{M_f} \right)^{d+1} \frac{M}{M_f}. \quad (2)$$

Naturally, black holes with mass of about the new fundamental mass $M_{BH} \sim M_f$, have Schwarzschild radii of about the new fundamental length scale $L_f = 1/M_f$ (which justifies the use of the limit $R_H \ll R$).

As for $M_f \sim 1$ TeV this radius is $R \sim 10^{-4}$ fm, p-p-collisions of $\sqrt{s} = 14$ TeV at the LHC, which allow for very hard (say: $\Delta p = 1$ TeV) parton-parton two-body scattering events, (Di-Jets of $E_{DiJet}^{Tot} \sim 1$ TeV) will, due to the uncertainty relation, yield two partons with impact parameters closer together than $\Delta x = \frac{1}{10000}$ fm. This corresponds to the Schwarzschild radius of the two partons with $M > 1$ TeV, close to the new fundamental scale $M_f \sim 1$ TeV - black holes can be created at the LHC in the ADD model!

The LXD-black hole production cross section can be approximated by the classical geometric cross-section

$$\sigma(M) \approx \pi R_H^2, \quad (3)$$

which only contains the fundamental Planck scale as coupling constant. This classical cross section is under debate ^{26,27}, but seems justified at least up to energies of $\approx 10M_f$ ²⁸.

Semi classical considerations yield form factors of order one²⁹, which take into account the fact that not the whole initial energy can be captured behind the Schwarzschild horizon. The naive classical result remains valid also in string theory ³⁰.

4 *H. Stöcker*

Angular momentum $J \approx 1/2Mb$ considerations change the results by a factor 2³¹. The black hole also carries charge, which gives rise to the exciting possibility of naked singularities²⁰.

What is the threshold for the black hole formation? From Thorn's General Relativistic arguments, two point like particles in a head on collision with zero impact parameter will *always* form a black hole, no matter how high or low their energy. At low energies, however, this overlap is improbable due to the spread of the wave functions by the uncertainty relation. This results in a necessary minimal energy to allow for the required close approach. Also this threshold is of order M_f , though the exact value is unknown - quantum gravity effects should play an important role for the wave functions of the colliding particles.

Setting $M_f \sim 1\text{TeV}$ and $d = 2 - 7$ one finds $\sigma \sim 400 \text{ pb} - 10 \text{ nb}$. Using the geometrical cross section formula, it is now possible to compute the differential cross section $d\sigma/dM$ which is given by summation over all possible parton interactions and integration over the momentum fractions, where the kinematic relation $x_1 x_2 s = \hat{s} = M^2$ has to be fulfilled. This yields

$$\frac{d\sigma}{dM} = \sum_{A_1, B_2} \int_0^1 dx_1 \frac{2\sqrt{\hat{s}}}{x_1 s} f_A(x_1, \hat{s}) f_B(x_2, \hat{s}) \sigma(M, d). \quad (4)$$

A numerical evaluation²¹ using the CTEQ - tables results in the differential cross section displayed in Figure 1, left. Most of the black holes created have masses close to the production threshold. This is due to the fact that at high collision energies, or small distances, respectively, the proton contains a high number of small x , low energy gluons and the total energy is distributed among them.

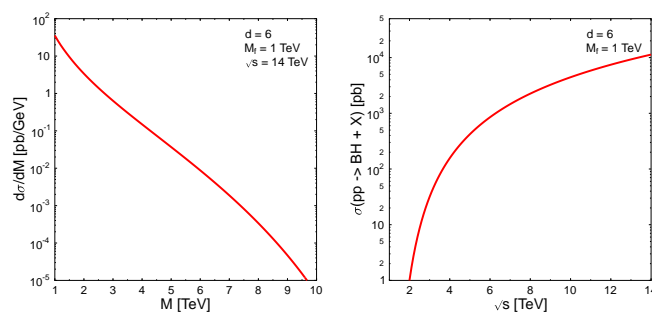


Fig. 1. The left plot shows the differential cross section for black hole production in proton-proton-collisions at the LHC for $M_f = 1 \text{ TeV}$. The right plot shows the integrated total cross section as a function of the collision energy \sqrt{s} . In both cases, the curves for various d differ from the above depicted ones by less than a factor 10.²¹

It is now straightforward to compute the total BH- cross section by integration over Eq. (4), see Figure 1, which yields a production cross section of about 10

nanobarn. $N_{\text{BH}} = 10^9$ black holes may be created at the LHC per year with the estimated full LHC luminosity $L = 10^{34} \text{cm}^{-2} \text{s}^{-1}$ at $\sqrt{s} = 14$ TeV: About one black hole per second would be created⁵.

LXD- Black Hole production would have dramatic consequences for future collider physics: Once the collision energy crosses the threshold for black hole production, no further information about the structure of matter at small scales can be extracted - this would be "the end of short distance physics"⁸.

3. Suppression of high mass correlated Di-Jet Signals - LXD-Black Hole Formation at the LHC

The above findings led to a high number of publications on the topic of TeV-mass black holes at colliders^{5,7,8,9,10,17,18}, for hadronic collisions as well as for heavy ion collisions¹⁹:

Per PbPb event, the number of BHs is increased (compared to pp) more than thousandfold as there are about 200-400 p-n collisions at a central ($b \sim 3$ fm) impact parameter event, which occurs with 400 mb cross section.

But how can we observe with certainty such a rare, exotic process, in the enormous background of a billion p-p events or so?

Are there unambiguous BH-observables, so robust and unique that an experimental signal is achievable? **Yes: Di-Jets vanish above M_f ! Therefore:**

$$\begin{aligned} &\text{IF (LXD-Black Holes at 14 TeV in pp @ LHC)} \\ &\text{.THEN.} \\ &\text{(No High pT-events, no } 2 \cdot 500 \text{ GeV Di-Jets @ LHC)} \end{aligned} \quad (5)$$

The first, cleanest signal for LXD-BH- formation at the LHC is the complete suppression of high energy back-to-back- correlated Di-Jets with $M > M_f$: those two very high energy partons, $E_{jet} \approx$ one-half M_f each, i.e. $p_t \geq 500$ GeV each, which usually define the Di-Jets in the standard model, now end up inside the black hole, instead of being observable in the detector! Di-Jets with $E_{Dijet} > M_f$ can not be emitted! A clean signature for BHs, indeed: The end of short distance physics.

The threshold cut-off due to black hole production, at $M \leq 1$ TeV or so in the transverse momentum spectra, also seems to lead to a decrease in the single particle spectra at higher p_t -values, above $p_t = 1$ TeV^{17,32}.

However, the high p_t - single particle spectra at high M may be filled up again due to Hawking radiation Mono-Jets, as discussed in the next paragraph. Therefore, the Di-Jet Suppression proposed here as signals for LXD-BHs, is the preferred observable.

In analogy to Heckler and Kapusta (3+1-dim BHs), Anchordoqui and Goldberg¹⁸ show that, for LXD-BH- Hawking radiation, emitted partons are closely spaced outside the Schwarzschild horizon. Hence, the partons do not fragment into hadrons, as strings in vacuum would, but they form a quark-gluon- (plus lepton- & EW-gauge vector boson-) plasma.

6 *H. Stöcker*

Above the temperature of the electroweak phase transition, i.e. at hundred GeV, even EW-particles melt in the superhot medium - like rhos in the QCD plasma - and can emit dilepton pairs at the Z 's in-medium mass.

Final thermal hadron freeze out then occurs only after isentropic hydrodynamical flow, at much lower temperatures, far from the horizon, i.e. at temperatures of the QCD phase transition scale, $T=200$ MeV.

The energy spectrum of the particles emerging from the "chromosphere" is found to be relatively soft: hard hadronic jets are almost entirely suppressed. The Jets are replaced by an isotropic distribution of soft photons and hadrons, with hundreds of particles in the few GeV range. This distinctive signature for black hole events at LHC should easily be discovered in the ALICE TPC.

4. Hard, Isotropic Multiple Monojet Emission as Signal for Hot LXD- Black Hole Hawking- Evaporation

Once produced, the black holes may undergo an evaporation process³³ whose thermal properties carry information about the parameters M_f and d . An analysis of the evaporation will therefore offer the possibility to extract knowledge about the topology of our space time and the underlying theory.

The evaporation process can be categorized in three characteristic stages^{8,10,34}:

- (1) BALDING PHASE: In this phase the black hole radiates away the multipole moments it has inherited from the initial configuration, and settles down in a hairless state. During this stage, a certain fraction of the initial mass will be lost in gravitational radiation.
- (2) EVAPORATION PHASE: The evaporation phase starts with a spin down phase in which the Hawking radiation carries away the angular momentum, after which it proceeds with emission of thermally distributed quanta until the black hole reaches Planck mass. The radiation spectrum contains all SUSY- and Standard Model particles, which are emitted on our brane, as well as gravitons, which are also emitted into the extra dimensions. It is expected that most of the initial energy is emitted in during this phase in Standard Model particles.
- (3) PLANCK PHASE: Once the black hole has reached a mass close to the Planck mass, it falls into the regime of quantum gravity and predictions become increasingly difficult. It is generally assumed that the black hole will then either completely decay in a few Standard Model particles or a stable (charged or neutral) Black Hole Remnant (BHR) will be left, which carries away the remaining energy and mass.

To understand the proposed signature caused by black hole production, namely the occurrence of multiple Monojets, in those Di-Jet suppressed events, we have to examine the Hawking- evaporation process in detail. The evaporation rate dM/dt also in higher dimensional space-times can be computed using the thermodynamics

of black holes. One finds for the BH-Hawking-like temperature the relation

$$T = \frac{1+d}{4\pi} \frac{1}{R_H} \quad , \quad (6)$$

where R_H is a function of M by Eq. (2). The smaller the black hole, the larger is its temperature.

Hence, the very hard radiation of the exploding, tiny black holes is a second signature.

Typical temperatures at the end of the lifetime are several hundred GeV. Since most of the particles of the black body radiation are emitted with ~ 100 GeV average energy, we can estimate the total number of emitted particles to be of order 10-100. This high temperature results in a very short lifetime such that the black hole will decay close to the primary interaction region and can be interpreted as a metastable intermediate state.

Integrating the thermodynamic identity $dS/dM = 1/T$ over M yields the entropy

$$S(M) = 2\pi \frac{d+1}{d+2} (M_f R_H)^{d+2} \quad . \quad (7)$$

For the number density of the states one has to take into account that for the typical collider-produced black hole. The emission of one particle will have a non-negligible influence on the total energy of the black hole. This problem can appropriately be addressed by including the back-reaction of the emitted quanta as has been derived in ^{35,36}. It is found that in the regime of interest here, when M is of order M_f , the emission rate for a single particle microstate is modified and given by the change of the black hole's entropy

$$n(\omega) = \frac{\exp[S(M-\omega)]}{\exp[S(M)]} \quad . \quad (8)$$

For Boltzmann-statistic this leads then to the spectral energy density

$$\varepsilon = \frac{\Omega_{(d+3)}}{(2\pi)^{3+d}} e^{-S(M)} \sum_{j=1}^{\infty} \frac{1}{j^{d+4}} \int_0^M e^{S(x)} (M-x)^{3+d} dx \quad , \quad (9)$$

where the value of the sum is given by a ζ -function. From this we obtain the evaporation rate

$$\frac{dM}{dt} = \frac{\Omega_{(d+3)}^2}{(2\pi)^{d+3}} R_H^{2+d} \zeta(4+d) e^{-S(M)} \int_0^M (M-x)^{(3+d)} e^{S(x)} dx \quad . \quad (10)$$

A plot of this quantity vs. M for various d is shown in Figure 2, left. The time-dependence of the mass is shown in Figure 2, right. We see that the evaporation process of 10 TeV BHs slows down in the late stages and enhances the lifetime of the black hole ¹⁰. The predominantly produced "light" primary BHs, $m_{BH}^{initial} \approx 1$ TeV, exhibit larger lifetimes. In case of stable Black Hole Remnants (BHRs), the lifetime will approach infinity - they will behave as a new kind of elementary particle with $M_{BHR} \sim M_f$, which can absorb mass (e.g. protons), but evaporates that mass

8 *H. Stöcker*

swiftly in form of photons and lepton pairs and decays then back into the BHR-groundstate.

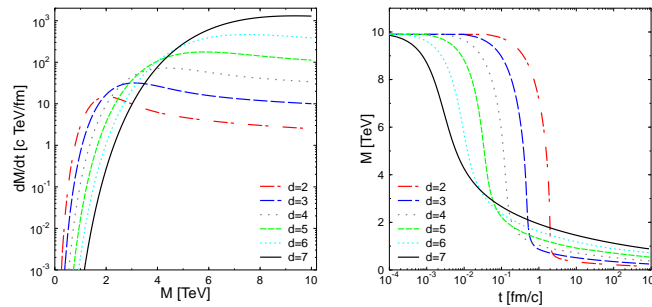


Fig. 2. The left plot shows the black hole’s evaporation rate in as a function of the initial mass for various d . The right plot shows the time evolution of the mass of a black hole with an initial mass of 10 TeV.

To perform a realistic simulation of the evaporation process, one has to take into account all Standard Model particles. In the extra dimensional scenario, SM particles are bound to our submanifold, whereas the gravitons are allowed to enter all dimensions. It has been argued that black holes emit mainly on the brane⁷. A very thorough description of these evaporation characteristics has been given in³⁷ which confirms the expectation that the bulk/brane evaporation rate is of comparable magnitude but the brane modes dominate.

For recent reviews on TeV-scale black holes see also³⁸ and references therein. Several experimental groups have included LXD- BH searches into their research programs for physics beyond the Standard Model, in particular the ALICE-, ATLAS- and CMS- Collaborations at the LHC³⁹. Both the PYTHIA 6.2⁴⁰ and the CHARYBDIS⁴¹ event generators allow for a simulation of black hole events and data reconstruction from the decay products. Such analysis has been summarized in Ref.⁴² and Ref.⁴³, respectively.

Ideally, the energy distribution of the decay products allows for a determination of the temperature (by fitting the energy spectrum to the predicted shape) as well as of the total mass of the BH (by summing up all energies). This then will allow for a reconstruction of the scale M_f and the number of extra dimensions.

Due to the high energy captured inside the black hole, its decay will be spectacular. Its distinct features allow for a second, independent signature, which can be used for the BH detection: in the very same event sample, where high energy Di-Jets are suppressed, a very high multiplicity of high energy Mono-Jets, much higher multiplication than in SM processes can be observed.

Furthermore, the thermally evaporating black hole yields a nearly isotropic decay pattern, with a high sphericity of the event.

5. Heckler-Kapusta-Hawking SM+SUSY-Plasma - above the electroweak phasetransition, formed in $pp \rightarrow BH$ reactions at the LHC

The energy density of the multiple Hawking Mono-Jets emitted from the evaporating BHs and BHRs produced in pp-collisions is enormous: Several TeV are emitted within a 4-Sphere of $\sim 10^{-12}\text{fm}^4/c$, implying energy densities of $\geq 10^9 \text{TeV fm}^{-3}$, i.e. many orders of magnitude higher than the energy densities expected for the Quark-Gluon Plasma $e \sim 500 \text{GeV fm}^{-3}$ to be created in Pb-Pb - collisions at the LHC at $\sqrt{s} = 5.5 \text{ATeV}$.

Hence the question arises whether - at this enormous energy density - the multiple jets thermalize to form a ultra-hot $T \gg T_{EW} \gg T_{QCD}$ Plasma of Standard-Model plus SUSY-particles.

Such a "hot Heckler-Kapusta-Hawking Plasma" scenario has been studied intensively for primordial 3-1-dimensional Black Holes in old cosmic radiation components by Heckler-Kapusta and coworkers^{49,50,48}. For the LXD-BHs and BHRs to be studied at the LHC a similar process might happen: The HKH-plasma for $T \sim 1 \text{TeV}$ should contain many "massless" SM Particles; as T is above the electroweak phasetransition temperature, the bare masses of e.g. $W^{+/-}$ and Z as well as light supersymmetric partners may become accessible to experiment. The HKH-plasma and the multiple-mono-jet emission may be distinguished by Hanbury Brown Twiss (HBT-) two- and more particle correlation measurements of the source size and life time of the system.

Interesting questions to study are the properties of SM- and SUSY-particles (masses, width) in the hot ($T \gg T_{EW}$) medium, thermalization and viscosity of this SM-SUSY "state" of matter, hydrodynamic expansion, abundant emission of (otherwise rare) quarks (b, t) and leptons.

6. High Intensity Beams of Low Energy Protons as a potent Energy Source through Hawking-Radiation of Black Hole Remnants (BHRs)

Stable remnants could be used as catalysors to capture and convert, in accord with $E = mc^2$, high intensity beams of low energy baryons (p,n, nuclei), of mass $\sim 1 \text{AGeV}$, into photonic, leptonic and light mesonic Hawking radiation, thus serving as a source of energy with 90% efficiency (as only neutrinos and gravitons would escape the detector/reactor).

If BHRs (Stable Remnants) are made available by the LHC or the NLC and can be used to convert mass in energy, then the total 2050 yearly world energy consumption of roughly 10^{21}Joule can be covered by just ~ 10 tons of arbitrary material, converted to radiation by the Hawking process via $m = E/c^2 = 10^{21}\text{J}/(3 \cdot 10^8\text{m/s})^2 = 10^4 \text{kg}$ ⁵¹.

7. Formation of stable Black Hole Remnants and Single Track Detection in the ALICE-TPC

Numerical simulations have so far assumed mostly that the black holes decay completely into SM- particles. From a theoretical point of view, however, there are strong indications that the black holes do not evaporate completely, but rather leave a meta-stable black hole remnant, dubbed Black Hole Remnant (BHR) or relic^{44,45} - do these relics leave the detector? Do they still emit radiation?

Fig. 3 shows that this is not the case: the mass evolution of the produced black holes stabilizes rapidly, $t < 1\text{fm}/c$, the average energy of emitted particles drops to zero within 10 fm.

The numerical results obtained (using the black hole event generator CHARYBDIS and the observables computed within the PHYTHIA environment) agree very well with the analytically computed results.

The fast convergence of the black hole mass is due to the fact that the spectral energy density has a maximum at energies $\sim 3T$. If the mass of the black hole decreases, emission of high energy particles is no longer possible because of energy conservation.

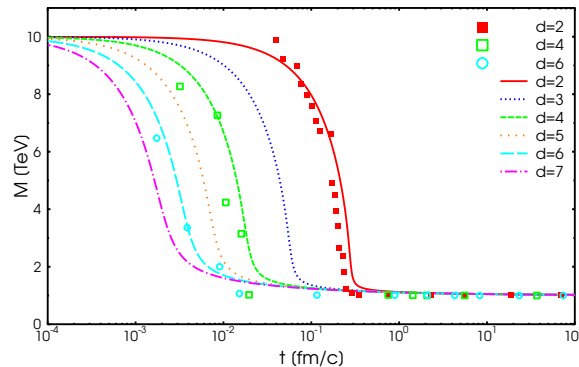


Fig. 3. The mass evolution for a black hole of initial mass $M = 10$ TeV and various d . Here, we set $M_R = M_f = 1$ TeV.

Figure 4 shows the p_T -spectrum after fragmentation as predicted by the CHARYBDIS-code. One clearly sees the additional contribution from the final decay, which causes a bump in the spectrum. This bump is absent in the case of remnant formation. This graph does not include background, but the ALICE detector can differentiate LXD-BHs from QCD-Background⁴⁶. Moreover, the microcanonical Hawking-Evaporation produces Multiple Mono-Jets even when BHRs are assumed. The BHR-remnant signal in p(14 TeV)p @ ALICE is clearly distinguishable from

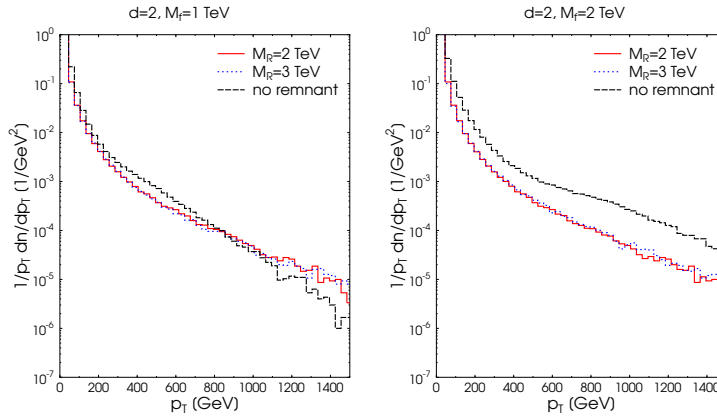


Fig. 4. Transverse momentum distribution after fragmentation with final (two-body) decay in contrast to the formation of a black hole remnant.⁴⁷

disappearing BHs!

Figure 5 displays the total multiplicities in such an event: when a black hole remnant is formed, the total multiplicity in CHARYBDIS is increased in spite of the fact that less energy is available (due to the missing BHR-mass) due to the many additional low energetic particles that are emitted in the late stages, instead of a final decay with 2 – 5 hard particles.

Note that this multiplicity increase is not an effect of the remnant formation itself, but rather it stems from the treatment of the decay in the microcanonical ensemble used in the present calculation: the black hole remnant, BHR, evaporates more particles with lower energy. The effect of hanced production of moderate energy secondaries will be stronger even if the Multi-Jets thermalize and form a QGP which then expands and cools.

Charged Black Hole Remnants should be observable in the TPC of the ALICE-Detector at the LHC as a magnetically very stiff single - or double charged track of very high momentum, large mass, moderate velocity.

8. Di-Jet-suppression in Relativistic Heavy Ion Collisions: formation of dense Quark-Gluon Matter at RHIC and LHC?

Remarkably strong bulk elliptic flow patterns of Dense Quark Matter have been observed at the Relativistic Heavy Ion Collider RHIC at BNL, N.Y. Even stronger collective effects are expected in Heavy Ion Collision. Apparently the pressure of the matter formed at RHIC is very high, $P_{QCD} \gg 1\text{GeV}/\text{fm}^3$! The elliptic V_2 -Flow is THE Barometer for the Equation of State.

Di- Jet suppression have been observed - about 50% can be attributed to Hadron Rescattering⁵². pQCD shows high opacity of QCD-matter to Di-Jets: only Monojets are emitted!

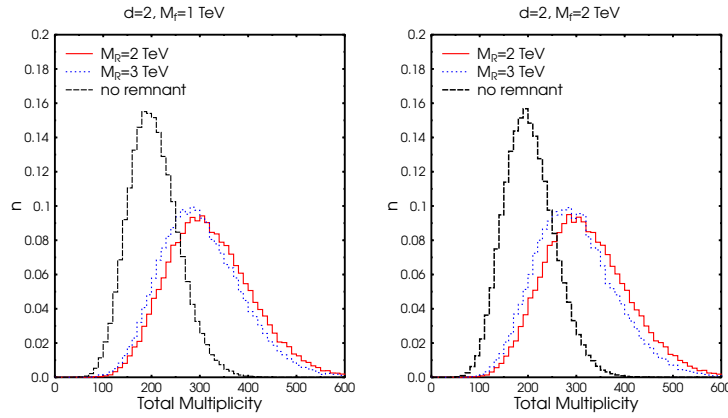


Fig. 5. Total multiplicity with final (two-body) decay and with formation of a black hole remnant for $d = 2$.⁴⁷

Are Mach-Cones or Wakes caused by Di-Jets in QGP MATTER observed!? The speed of sound, c_s , is the response to jet-penetration probes - weakens can lead the measurement of dispersion relations. Transport coefficients (viscosity, conductivity) can be determined.

At RHIC huge $\langle v_2 \rangle$ of high p_t particles is observed! The QG-Plasma Pressure is much larger than the Hadron Pressure ! Therefore, QUARK MATTER FLOWS! QGP is early-on thermalized - and can create huge Plasma pressure!

Ultra-dense QCD matter can be discovered with heavy ions in the LHC -just like at RHIC- through three steps:

1. P_{QCD} : remarkable bulk elliptic flow patterns, $v_2 > 30\%$
2. pQCD: higher opacity to Di-Jets, tomography even for high p_t -jets
3. c_s : response to penetrating probes, Mach-Cones and Tsunami emission.

Parton energy loss studies in pQCD show that the dominant mechanism is gluon bremsstrahlung after collisions in the medium. The scattering power of the QCD medium is proportional to the "gluon density" and hence to the gluonic $T_{\mu\nu}$. But up to now $3 \Leftrightarrow 2$ gluon collisions have not yet been incorporated, however, see Xu and Greiner⁵³! Therefore, for Jet Quenching and Tomography of Quark Gluon Matter at RHIC: (Gyulassy, Vitev, Wang⁵⁴) one needs very large gluon densities! Jet Quenching in medium has been discovered at RHIC, but not understood.

How much jet quenching is due to Hadrons FSI ? Jets interact in both, Plasma- and Hadron Phase!

Hadronic rescattering - responsible for 50% energy loss?⁵²

An additional 50% of p_T -suppression is due to hadron rescattering: the expansion of small color transparency configuration yields 50% hadronic quenching, an additional $\sim 50\%$ QGP is needed.

Also here, half of the effect is due to hadronic, half due to partonic interaction⁵². How much of the suppression of Di-hadron correlations is due to hadronic FSI (final state interactions)?

9. Mach Shock Cones and nonlinear Tsunamis induced by Jets Stopping in Quark-Gluon Plasma

Sideward peaks have been recently observed^{55,56,57,58,59} in azimuthal distributions of secondaries associated with a high p_T hadron in central Cu+Cu and Au+Au collisions at $\sqrt{s_{NN}} = 62$ and 200 GeV. Experimental data of the STAR and PHENIX collaborations both show that the "away-side" dip of two-hadron correlations at $\Delta\phi = \pi$ disappears for peripheral events and with raising the transverse momentum of the associated particle.

In Ref.⁶⁰ such peaks were predicted as a signature of Mach shocks created by partonic jets propagating through a quark-gluon plasma (QGP) formed in a heavy-ion collision. Analogous Mach shock waves were studied previously in cold nuclei^{61,62,63,64,65}. This phenomenon has subsequently been studied in a numerical Ref.⁶⁶ linearized fluid-dynamical approach.

Other possible explanations of the sideward peaks in the Mono-jet distributions have been offered⁶⁷. For example, it is argued in Refs.^{60,68} that Mach-like motions of quark-gluon matter can appear via the excitation of collective plasmon waves, "wakes", by the moving color charge associated with the leading jet.

A similar mechanism, electron emission induced by heavy-ion irradiation of metal foils, was predicted in Ref.⁶⁹. Later on this effect was observed experimentally⁷⁰.

Keep in mind that the colored plasmon waves can be produced only in a nonideal QGP⁶⁸. According to Refs.^{71,72}, excitation of transverse plasmon waves in QGP may lead to a conical, Cherenkov-like emission of particles. However, this is possible only for a strongly coupled QGP.

A high energy parton moving in the storm of moving quark-gluon matter deposits a fraction of the parton's energy and momentum along its trajectory. Colorless sound waves then produce the Mach region of perturbed collective flow behind the leading particle.

In the fluid rest frame (FRF) the Mach region has a conical shape with an opening angle (with respect to the direction of particle propagation) given by the expression

$$\theta_M = \sin^{-1} \left(\frac{c_s}{\tilde{v}} \right), \quad (11)$$

where c_s denotes the sound velocity of the unperturbed fluid and \tilde{v} is the particle velocity with respect to the fluid.

This Mach-Cone can be formed only if $\tilde{v} > c_s$. Strictly speaking, Eq. (11) is applicable only for weak, sound-like linear perturbations.

Following Refs.^{60,66} one can estimate the angle of preferential emission of partonic or hadronic secondaries associated with a fast jet in the QGP.

The appearance of the Mach shock leads to angular maxima in the particle emission, corresponding to $|\Delta\phi - \pi| = \pi/2 - \theta_M$. In the case of ideal QGP ($c_s = 1/\sqrt{3}$), substituting $\tilde{v} \simeq 1$ into Eq (11), one obtains that $\Delta\phi \simeq \pi \pm 0.96$.

This agrees well with positions of maxima of the two-particle distributions observed in heavy-ion collisions at RHIC energies. Therefore, by measuring the two-particle angular distributions, one should be able to easily extract the sound velocity of the QGP.

These estimates correspond to the idealized case of homogeneous, infinite, static matter.

However, the systems are finite, and collective expansion flow is known to be strong in relativistic collisions of heavy nuclei⁷³.

For example, thermal fits of RHIC data give for most central events the average radial flow velocities $u_f \sim 0.6$. This value is as large as c_s in the deconfined phase!

Due to the hadronization effects, c_s will be strongly time-dependent. Characteristics of Mach shocks in expanding quark-gluon matter have been considered in Refs.^{74,75}

Typical flow parameters at RHIC and LHC energies yield⁷⁴ shapes and orientation of Mach regions which are strongly modified as compared to the case of static medium.

Especially strong deformation of Mach-Cones takes place when the flow velocity is orthogonal to the direction of the jet's propagation. In this case the collective flow acts like a storm, deflecting the Mach-Cone in the direction transversal to the di-jet axis.

As a result, the shape of Mach region becomes asymmetric with respect to the jet trajectory in the global center of mass frame (CMF).

This is illustrated in Fig. 6. The insert shows that the boundaries of Mach region have different angles, $\theta_+ \neq \theta_-$, with respect to the jet velocity \mathbf{v} in the CMF. By using the Lorentz transformation from CMF to FRF, the following formulae is obtained for θ_{\pm} in the weak shock approximation:

$$\tan \theta_{\pm} \simeq \gamma_u \frac{\gamma_s c_s \pm \gamma_u u}{1 \mp \gamma_s c_s \gamma_u u}, \quad (12)$$

where $\gamma_u = (1 - u^2)^{-1/2}$, $\gamma_s = (1 - c_s^2)^{-1/2}$. One can see that for small flow velocities the difference of the Mach angles θ_{\pm} in moving and static matter is approximately linear in u .

Figure 7 shows the numerical values of the Mach angles for an ultrarelativistic jet moving through the QGP transversely to its flow velocity. The solid and dashed curves are calculated by using Eq. (12) with $c_s = \sqrt{1/3}$. The dashed-dotted and dotted lines represent the corresponding angles for $c_s = \sqrt{2/3}$.

To discuss possible observable effects, below we consider properties of the Mach shock created by high-energy jets propagating in a cylindrical volume (fireball) of

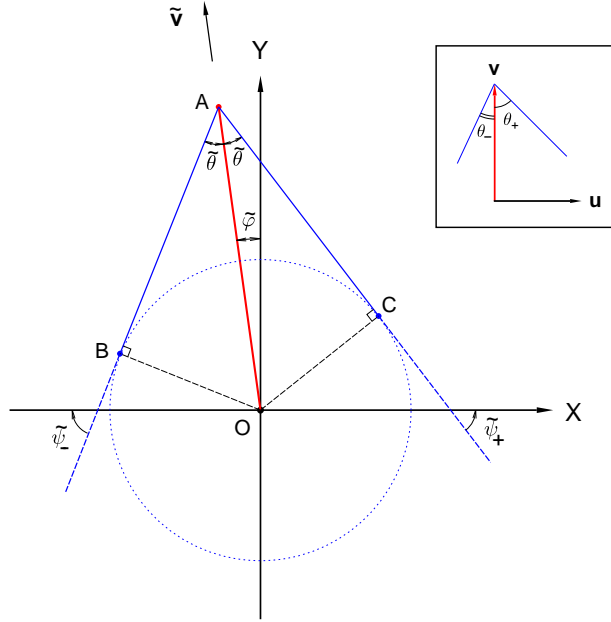


Fig. 6. Mach region created by jet moving with velocity \mathbf{v} orthogonal to the fluid velocity \mathbf{u} . The main plot and the insert correspond to FRF and CMF, respectively. It is assumed that jet moves from O to A in FRF. The dotted circle represents the front of sound wave generated at point O .

the QGP expanding in radial directions. For simplicity we consider the case when both trigger and away-side jets have zero pseudorapidities in CMF. Presumably, this picture corresponds to the most central collisions of equal nuclei. In Fig. 8 we schematically show events with different positions of di-jet axes $A_i B_i$ ($i = 1, 2, 3$) with respect to the center of the fireball. In the $2 - 2'$ event, the away-side jet '2' propagates along the diameter $A_2 B_2$, i.e. collinearly with respect to the collective flow. In the two other cases, the di-jet axes are oriented along the chords, $A_1 B_1$ and $A_3 B_3$, respectively. In such events, the fluid velocity has both transverse and collinear components with respect to the jet axis. In Fig. 8 we also show how the Mach fronts will be deformed in expanding matter.

The radial expansion of the fireball gives rise to the shift of sideward peaks of the $\Delta\phi$ distributions. This leads to an additional broadening of the away-side maxima of the two-particle correlation function. On average over events with different position of di-jet axes, the peaks will be distributed in the angular interval⁷⁴

$$\delta\phi \simeq \langle \theta_+(|u_x|) - \theta_-(|u_x|) \rangle \simeq \theta_+(\langle u_x \rangle) - \theta_-(\langle u_x \rangle). \quad (13)$$

In the second equality a linear dependence of θ_{\pm} on the transverse component of flow velocity $|u_x|$ was assumed. Using the results of Fig. 7 for the case $c_s = 1/3$ we get the azimuthal distance between the peaks of about 110° and the angular spread

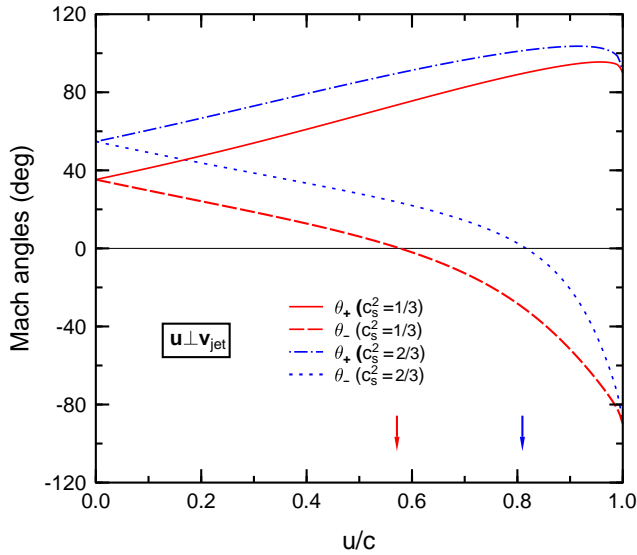


Fig. 7. Angles of Mach region created by a jet moving transversely to the fluid velocity \mathbf{u} in the CMF. Lower (upper) set of curves corresponds to the case $c_s^2 = 1/3$ ($2/3$). Arrows mark the values $u = c_s$.

of emitted hadrons, $\delta\phi$, in the range $25^\circ - 50^\circ$ for $\langle u_x \rangle = 0.2 - 0.4$. This agrees quite well with the positions and widths of the sideward peaks observed by the STAR and PHENIX collaborations^{55,56,57,58}. On the other hand, the choice $c_s^2 = 2/3$ gives approximately the same values of $\delta\phi$, but the predicted angular difference between two peaks is too small, only about 70° . On the basis of this analysis we conclude that in individual events the sideward maxima should be located asymmetrically with respect to $\Delta\phi = \pi$ and they will be narrower than in an ensemble of different events. These effects can be observed by measuring three-particle correlations.

The STAR-collaboration reports to see no effect of a Mach-Cone in three particle correlations: is this due to the deflection of the jets due to tsunami-like flow of the underlying exploding plasma phase?

Distinctive features of conical flow are studied in present data with different p_T windows. How can there be a perfect fluid, ideal hydrodynamic flow, but no sound waves? They must be there, if the matter is ideal fluid-like!

PHENIX reports exactly the opposite finding of STAR: strong signs of Mach-Cones observed in the three particle correlations at the away-side jet!

The deformations of quark-gluon- Mach-Cones by underlying collective flow due

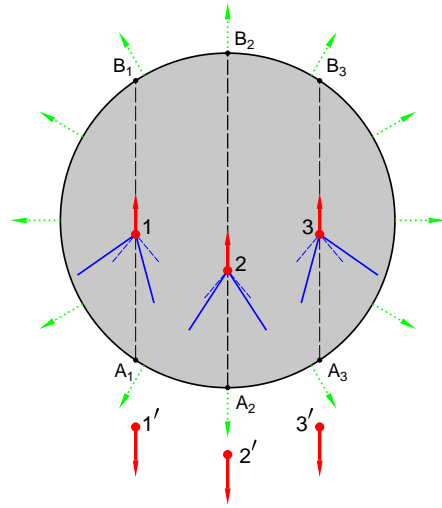


Fig. 8. Schematic picture of Mach shocks from jets 1, 2, 3 propagating through the fireball matter (shaded circle) created in a central heavy-ion collision. Dotted arrows represent local velocities of fireball expansion. Thick downward arrows show associated trigger jets. The Mach shock boundaries are shown by solid lines. Short-dashed lines give positions of shock fronts in the case of static fireball.

to the high Pressure, P_{QCD} , of the QGP follows the following four steps:

1. Collective flow of Plasma yields
2. Deformation of Mach-Cone leading to
3. Deflection of it's axis in the flow direction, resulting in
4. Away-side angular satellites being skewed and broadened

The Mach shock cones are shifted in the expanding QGP fluid. These shifts could be directly visible in 3-particle correlations, and in the broadening of the away-side maxima.

10. LXD-BHs in Pb+Pb-collisions at Colliders

The geometrical increase of the (event-by-event) LXD-BH-production probability for heavy ion collision can be as large as tenthousandfold at the LHC, due to impact parameter - and participant number increase. Hence, the interaction of the LXD-BHs, their remnants and their secondary Hawking-Radiation with the primary medium (quark-gluon plasma) generated by the bulk of the softer QCD interactions in the Pb+Pb collisions may be probed: In particular, secondary Mach

18 *H. Stöcker*

shock waves caused by the Hawking Monojets, secondary hydrodynamic explosions of the Heckler-Kapusta-Hawking Plasma inside the "soft" QGP of the ion-ion collision, and the propagation of these density waves through the Plasma deserve further studies⁷⁶.

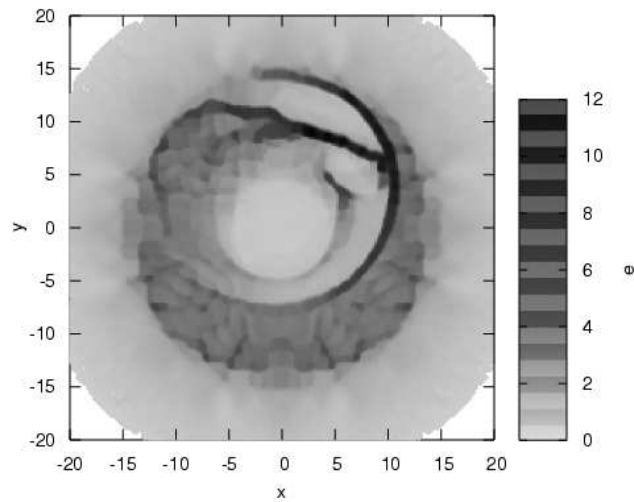


Fig. 9. Mach Shock "cones" left by "slowly" moving source of high energy density "secondary" Plasma, generated by either stopped QCD-Jets or by a secondary Heckler-Kapusta-Hawking Plasma surrounding a Black Hole created in Pb+Pb ($\sqrt{s} = 5.5$ TeV) collisions, K. Paech, priv. communication

11. Conclusion

The LHC will provide exciting discovery potential way beyond supersymmetric extensions of the SM!

Acknowledgements

This work has been supported by FIAS, GSI, BMBF, DFG, DAAD, DOE, RIKEN, by the Alexander von Humboldt-Stiftung, and by the ALICE collaboration.

Discussions with and important contributions by the following colleagues are acknowledged:

Barbara Betz, Leonid Satarov, Igor Mishustin, Harry Appelshäuser, Peter Braun-Munzinger, Adrian Dumitru, Ben Koch, Marcus Bleicher, Sabine Hossfelder, Carsten Greiner, Tom Humanic, Kerstin Paech, Dirk Rischke, Mike Strickland, Wolfgang Cassing, Walter Greiner, Yasushi Nara, Daniel Henkel, Vesa Ruuskanen, Kari Eskola, Ed Shuryak, Johanna Stachel.

References

1. K. Schwarzschild, Sitzungsberichte der Deutschen Akademie der Wissenschaften zu Berlin, Klasse für Mathematik, Physik und Technik, 189 (1916)
2. I. Antoniadis, Phys. Lett. B **246**, 377 (1990); I. Antoniadis and M. Quiros, Phys. Lett. B **392**, 61 (1997); K. R. Dienes, E. Dudas and T. Gherghetta, Nucl. Phys. B **537**, 47 (1999); K. R. Dienes, E. Dudas and T. Gherghetta, Phys. Lett. B **436**, 55 (1998).
3. N. Arkani-Hamed, S. Dimopoulos and G. R. Dvali, Phys. Lett. B **429**, 263 (1998); I. Antoniadis, N. Arkani-Hamed, S. Dimopoulos and G. R. Dvali, Phys. Lett. B **436**, 257 (1998); N. Arkani-Hamed, S. Dimopoulos and G. R. Dvali, Phys. Rev. D **59**, 086004 (1999).
4. L. Randall and R. Sundrum, Phys. Rev. Lett. **83**, 4690 (1999). and Phys. Rev. Lett. **83**, 3370 (1999).
5. S. Dimopoulos and G. Landsberg, Phys. Rev. Lett. **87**, 161602 (2001); P.C. Argyres, S. Dimopoulos, and J. March-Russell, Phys. Lett. **B441**, 96 (1998).
6. T. Banks and W. Fischler, arXiv:hep-th/9906038.
7. R. Emparan, G. T. Horowitz and R. C. Myers, Phys. Rev. Lett. **85**, 499 (2000).
8. S. B. Giddings and S. Thomas, Phys. Rev. D **65** 056010 (2002).
9. K. M. Cheung, Phys. Rev. Lett. **88**, 221602 (2002); Y. Uehara, [arXiv:hep-ph/0205068]; Prog. Theor. Phys. **107**, 621 (2002); L. Anchordoqui and H. Goldberg, Phys. Rev. D **67**, 064010 (2003);
10. S. Hossenfelder, S. Hofmann, M. Bleicher and H. Stöcker, Phys. Rev. D **66**, 101502 (2002).
11. S. Hossenfelder, M. Bleicher, S. Hofmann, H. Stoecker and A. V. Kotwal, Phys. Lett. B **566** (2003) 233 [arXiv:hep-ph/0302247].
12. R. Casadio and B. Harms, Phys. Rev. D **64** (2001) 024016 [arXiv:hep-th/0101154].
13. M. Cavaglia, S. Das and R. Maartens, Class. Quant. Grav. **20** (2003) L205 [arXiv:hep-ph/0305223].
14. S. Alexeyev, A. Barrau, G. Boudoul, O. Khovanskaya and M. Sazhin, Class. Quant. Grav. **19** (2002) 4431 [arXiv:gr-qc/0201069].
15. A. Bonanno and M. Reuter, Phys. Rev. D **62** (2000) 043008 [arXiv:hep-th/0002196].
16. M. Bleicher, S. Hofmann, S. Hossenfelder and H. Stöcker, Phys. Lett. **548**, 73 (2002); J. Alvarez-Muniz, J. L. Feng, F. Halzen, T. Han and D. Hooper, Phys. Rev. D **65**, 124015 (2002). I. Mocioiu, Y. Nara and I. Sarcevic, Phys. Lett. B **557**, 87 (2003). M. Cavaglia, S. Das and R. Maartens, Class. Quant. Grav. **20**, L205 (2003); M. Cavaglia and S. Das, Class. Quant. Grav. **21**, 4511 (2004).
17. A. Chamblin and G. C. Nayak, Phys. Rev. D **66**, 091901 (2002) [arXiv:hep-ph/0206060].
18. L. Anchordoqui and H. Goldberg, Phys. Rev. D **67** (2003) 064010 [arXiv:hep-ph/0209337].
19. S. Hofmann, M. Bleicher, L. Gerland, S. Hossenfelder, K. Paech and H. Stöcker, J. Phys. G **28** (2002) 1657.
20. R. Casadio and B. Harms, Int. J. Mod. Phys. A **17**, 4635 (2002); I. Ya. Yref'eva, Part.Nucl. 31, 169-180 (2000). S. B. Giddings and V. S. Rychkov, Phys. Rev. D **70**, 104026 (2004); V. S. Rychkov, [arXiv:hep-th/0410041]; T. Banks and W. Fischler, [arXiv:hep-th/9906038]. O. V. Kancheli, [arXiv:hep-ph/0208021].
21. S. Hossenfelder, arXiv:hep-ph/0510236.
22. A. Goyal, A. Gupta and N. Mahajan, Phys. Rev. D **63**, 043003 (2001); R. Emparan, M. Masip and R. Rattazzi, Phys. Rev. D **65**, 064023 (2002); D. Kazanas and A. Nicolaidis, Gen. Rel. Grav. **35**, 1117 (2003).
23. A. Ringwald and H. Tu, Phys. Lett. B **525** 135-142 (2002); J. Feng and A. Shapere,

20 *H. Stöcker*

- Phys. Rev. Lett. **88**, 021303 (2002); A. Cafarella, C. Coriano and T. N. Tomaras, [arXiv:hep-ph/0410358]; L. A. Anchordoqui, J. L. Feng, H. Goldberg and A. D. Shapere, Phys. Rev. **D 65** 124027 (2002); S. I. Dutta, M. H. Reno and I. Sarcevic, Phys. Rev. **D 66**, 033002 (2002).
24. K. Cheung, [arXiv:hep-ph/0409028]; G. Landsberg [CDF and D0 - Run II Collaboration], [arXiv:hep-ex/0412028].
 25. R. C. Myers and M. J. Perry Ann. Phys. **172**, 304-347 (1986).
 26. M. B. Voloshin, Phys. Lett. B **518**, 137 (2001); Phys. Lett. B **524**, 376 (2002); S. B. Giddings, in *Proc. of the APS/DPF/DPB Summer Study on the Future of Particle Physics (Snowmass 2001)* ed. N. Graf, eConf **C010630**, P328 (2001).
 27. V. S. Rychkov, Phys. Rev. **D 70**, 044003 (2004); K. Kang and H. Nastase, [arXiv:hep-th/0409099].
 28. S. N. Solodukhin, Phys. Lett. B **533**, 153 (2002); A. Jevicki and J. Thaler, Phys. Rev. **D 66**, 024041 (2002); T. G. Rizzo, in *Proc. of the APS/DPF/DPB Summer Study on the Future of Particle Physics (Snowmass 2001)* ed. N. Graf, eConf **C010630**, P339 (2001); D. M. Eardley and S. B. Giddings, Phys. Rev. **D 66**, 044011 (2002).
 29. H. Yoshino and Y. Nambu, Phys. Rev. **D 67**, 024009 (2003).
 30. G. T. Horowitz and J. Polchinski, Phys. Rev. **D 66** 103512 (2002).
 31. S. N. Solodukhin, Phys. Lett. **B 533** 153-161 (2002); D. Ida, K. Y. Oda and S. C. Park, Phys. Rev. **D 67**, 064025 (2003).
 32. L. Lonnblad, M. Sjö Dahl and T. Akesson, [arXiv:hep-ph/0505181].
 33. S. W. Hawking, Comm. Math. Phys. **43**, 199-220 (1975); Phys. Rev. **D 14**, 2460-2473 (1976).
 34. S. Hossenfelder, B. Koch and M. Bleicher, arXiv:hep-ph/0507140.
 35. D. N. Page, Phys. Rev. **D 13** 198 (1976); R. Casadio and B. Harms, Phys. Rev. **D 64**, 024016 (2001); Phys. Lett. **B 487** 209-214 (2000).
 36. P. Kraus and F. Wilczek, Nucl. Phys. B **433**, 403 (1995); P. Kraus and F. Wilczek, Nucl. Phys. B **437**, 231 (1995); E. Keski-Vakkuri and P. Kraus, Nucl. Phys. B **491**, 249 (1997); S. Massar and R. Parentani, Nucl. Phys. B **575**, 333 (2000); T. Jacobson and R. Parentani, Found. Phys. **33**, 323 (2003); M. K. Parikh and F. Wilczek, Phys. Rev. Lett. **85**, 5042 (2000).
 37. P. Kanti, Int. J. Mod. Phys. A **19** (2004) 4899.
 38. G. Landsberg, [arXiv:hep-ph/0211043]; M. Cavaglia, Int. J. Mod. Phys. A **18**, 1843 (2003); S. Hossenfelder, [arXiv:hep-ph/0412265].
 39. R. Barbera, B. Batyunya, Yu. Belikov, M. Botje, P. G. Cerello, A. Feliciello, T. Humanic, G. Lo Curto, A. Palmeri, F. Ruggi, ALICE Internal Note ALICE/ITS 98-06
 40. T. Sjöstrand, L. Lonnblad and S. Mrenna, [arXiv:hep-ph/0108264].
 41. C. M. Harris, P. Richardson and B. R. Webber, JHEP **0308**, 033 (2003) [arXiv:hep-ph/0307305].
 42. J. Tanaka, T. Yamamura, S. Asai and J. Kanzaki, [arXiv:hep-ph/0411095].
 43. C. M. Harris, M. J. Palmer, M. A. Parker, P. Richardson, A. Sabetfakhri and B. R. Webber, [arXiv:hep-ph/0411022].
 44. B. Koch, M. Bleicher and S. Hossenfelder, hep-ph/0507138.
 45. M. Bleicher, S. Hofmann, S. Hossenfelder and H. Stöcker, Phys. Lett. **B548**, 73 (2002).
 46. P. Cortese *et al.* [ALICE Collaboration], CERN-LHCC-2002-016
 47. B. Koch, M. Bleicher and S. Hossenfelder, JHEP **0510** (2005) 053 [arXiv:hep-ph/0507138].
 48. A. F. Heckler, Phys. Rev. **D 55** (1997) 480 [arXiv:astro-ph/9601029].
 49. J. I. Kapusta, Phys. Rev. Lett. **86** (2001) 1670-1673
 50. A. F. Heckler, Phys. Rev. Lett. **78** (1997) 3430 [arXiv:astro-ph/9702027].

51. H. Stöcker, Deutsches Patent- und Markenamt München, 10 2006 007 824.1-54
52. W. Cassing, K. Gallmeister and C. Greiner, *J. Phys. G* **30** (2004) S801 [arXiv:hep-ph/0403208].
53. Z. Xu and C. Greiner *Phys. Rev. C* **71**, 064901 (2005)
54. M. Gyulassy, I. Vitev, X. N. Wang and B. W. Zhang, arXiv:nucl-th/0302077.
55. C. Adler et al. (STAR Collab.), *Phys. Rev. Lett.* **90**, 082302 (2003).
56. C. Adler et al. (STAR Collab.), *Phys. Rev. Lett.* **C91**, 072304 (2003); hep-ph/0501016.
57. F. Wang (STAR Collab.), *J. Phys. G* **30**, S1299 (2004).
58. B. Jacak (PHENIX Collab), talk at Int. Conf. on Physics and Astrophysics of Quark Gluon Plasma, Kolkata, India, 2005.
59. H. Büsching (PHENIX Collab), talk at Int. Conf. Quark Matter 2005, Budapest, Hungary, 2005.
60. H. Stöcker, *Nucl. Phys.* **A750**, 121 (2005); nucl-th/0406018.
61. J. Hofmann, H. Stöcker, W. Scheid and W. Greiner, in Report of Int. Workshop on BeV/nucleon Collisions of Heavy Ions: How and Why, Bear Mountain, NY, 1974 (report BNL-AUI, 1975);
H.G. Baumgardt, J.U. Schott, Y. Sakamoto, E. Schopper, H. Stöcker, J. Hofmann, W. Scheid and W. Greiner, *Z. Phys.* **A273**, 359 (1975);
J. Hofmann, H. Stöcker, U. Heinz, W. Scheid and W. Greiner, *Phys. Rev. Lett.* **36**, 88 (1976).
62. H. Stöcker, J. Hofmann, J.A. Maruhn and W. Greiner, *Prog. Part. Nucl. Phys.* **4**, 133 (1980).
63. H. Stöcker and W. Greiner, *Phys. Rep.* **137**, 277 (1986).
64. G.F. Chapline and A. Granik, *Nucl. Phys.* **A459**, 681 (1986).
65. D.H. Rischke, H. Stöcker and W. Greiner, *Phys. Rev. D* **42**, 2283 (1990).
66. J. Casalderrey-Solana, E.V. Shuryak and D. Teaney, hep-ph/0411315;
E.V. Shuryak, talk at Int. Conf. Quark Matter 2005, Budapest, Hungary, 2005.
67. I. M. Dremlin, hep-ph/0602135v1
68. J. Ruppert and B. Müller, *Phys. Lett.* **B618**, 123 (2005).
69. W. Schäfer, H. Stöcker, B. Müller and W. Greiner, *Z. Phys.* **A288**, 349 (1978).
70. H.J. Frischkorn et al., *Phys. Lett.* **76A**, 155 (1980);
H.J. Frischkorn et al., *Phys. Rev. Lett.* **58**, 1773 (1987).
71. I. Dremin, *JETP Lett.* **30**, 140 (1979); hep-ph/0507167.
72. A. Majumder and X.-N. Wang, hep-ph/0507062;
V. Koch, A. Majumder and X.-N. Wang, hep-ph/0507063.
73. Nu Xu, *Prog. Part. Nucl. Phys.* **53**, 165 (2004).
74. L.M. Satarov, H. Stöcker and I.N. Mishustin, *Phys. Lett.* **B627**, 64 (2005).
75. T. Renk and J. Ruppert, hep-ph/0509036.
76. B. Betz et al., to be published.